# Analysis of the Indoor Broadband Power-Line Noise Scenario

José Antonio Cortés, Luis Díez and Francisco Javier Cañete

***Abstract*—Indoor broadband power-line noise is composed of three main terms: impulsive components, narrowband interferences and background noise. Most impulsive components have a cyclostationary behavior. However, while some of them consist of impulses of considerable amplitude, width and repetition rates of 50 Hz/100 Hz (in Europe), others have lower amplitude and shorter impulses and repetition rates of up to hundreds of kilohertz. Classical studies compute statistics of the impulse characteristics without taking into account these significant differences. This paper presents a detailed analysis of these noise terms with a clear distinction between their constituent terms. A classification of the narrowband interferences according to their power spectral density and their statistical behavior is also given. Finally, the instantaneous power spectral density of the background noise and its probability distribution are investigated.**

***Index Terms*—Impulsive noise, narrowband interferences, background noise, broadband power-line communications (PLC).**

## I. Introduction

In the last decade, there has been an increasing interest in the use of the power-line network for broadband communications purposes. In a first instance, the utilization of the low voltage distribution lines as a last-mile technology attracted significant attention from utility companies. However, the strong competition from digital subscriber lines (DSL) and cable services has discouraged the deployment of outdoor PLC systems in most developed countries. Paradoxically, this high penetration of DSL services has widened the possibilities of indoor PLC applications. Since the objective of these systems is to utilize the in-building power grid for computer and entertainment equipment interconnection, they are an appealing solution for the distribution of triple play services in small offices and homes.

As a result of the considerable research effort carried out in broadband PLC in the last years, there is a good understanding of the channel response characteristics [1], [2], and appropriate models for obtaining representative frequency responses have been proposed [3], [4], [5]. On the contrary, there are few works dealing with power-line noise characterization and modeling [2], [4], [6], [7], [8], [9]. Broadband power-line noise does not certainly follow the classical additive white Gaussian noise (AWGN) model. It has two main origins: noise generated by the electrical devices connected to the power grid and external noise coupled to the indoor network via radiation or via conduction. It is composed of the following terms [7]:

1) *Impulsive noise*. It comprises different components that can be also classified according to:
   a) *Periodic impulsive noise synchronous with the mains*. It is a cyclostationary noise, synchronous with the mains and with a frequency of 50 Hz/100 Hz in Europe. It is commonly originated by silicon controlled rectifiers (SCR) in power-supplies.
   b) *Periodic impulsive noise asynchronous with the mains*. It has been traditionally considered to be formed by periodic impulses with rates between 50 kHz and 200 kHz. However, repetition rates outside this range have been found in the measurements accomplished in this work. Moreover, in addition to these high repetition frequencies, this type of noise also exhibits an underlying period equal to the mains one, which allows to categorize it as cyclostationary.
   c) *Asynchronous impulsive noise*. It has an unpredictable nature, with no regular occurrence, and is mainly due to transients caused by the connection and disconnection of electrical devices. Due to its fitful appearance pattern, from now on it will be referred to as sporadic impulsive noise.
2) *Narrowband interferences*. They are mostly formed by sinusoidal or modulated signals with different origins: broadcast stations, spurious caused by electrical appliances with a transmitter or a receiver, etc. Their level usually varies with daytime and, as it will be shown in this work, in some cases they also vary synchronously with the mains. Hence, some of them can be also treated as cyclostationary.
3) *Background noise*. It encompasses the rest of noise types not included in the previous categories. It can be assumed to be cyclostationary, with a level that

depends on the number and type of electrical devices connected to the network.

At present time, there are still many unknowns related to the above noise terms. Regarding the background noise, its probability distribution and instantaneous power spectral density (PSD) is usually accomplished without discarding the impulsive components and the narrowband interferences. As a consequence, the resulting probability distribution is clearly non-Gaussian and a quite peaky PSD is obtained [4], [10]. Concerning the impulsive noise, its analysis has been mainly accomplished in the time-domain by means of a digital oscilloscope triggered by a peak detector output. The stored data is employed to compute statistics of the interarrival time, pulse width and pulse amplitude [7], [8]. However, this procedure does not take into account the different nature of the three constituent components of this noise term, e.g. it mixes periodic and aperiodic impulses. Moreover, in the periodic noise type, it does not distinguish between the synchronous and the asynchronous terms, which have quite diverse characteristics: periodic synchronous components usually have much higher amplitude and width than periodic asynchronous ones but, on the other hand, the latter have much higher repetition rates. In addition, the presence of the remaining noise terms in the captured data biases the estimation of the pulse width and amplitude. Hence, statistics computed in this way are of little use for the development of realistic noise models.

The aim of this paper is the characterization of the different noise terms. The employed methodology, which combines time-domain and frequency domain techniques, provides both pulse waveforms and repetition rates of the impulsive noise components. A classification of the narrowband interferences according to their PSD and their statistical characteristics, along with results on the probability distribution and the instantaneous PSD of the background noise are also given. Measurements employed in this work have been obtained from a campaign performed in three scenarios: in laboratories and offices of a university building, in an apartment of about 80 $m^2$ and in a detached house of about 300 $m^2$. The number of noise registers exceeds 50, with a similar number of them at the mentioned locations.

Results presented in this work are particularly helpful for the development of noise models to be employed in the design and optimization of digital communication systems. This is especially applicable to coding schemes, which must be particularly matched to the noise characteristics. Similarly, a good knowledge of the predictable characteristics of some noise components, e.g. periodic asynchronous impulsive ones, can be also employed in the optimization of modulation parameters and receiver structures [11].

The rest of the paper is organized as follows. Section II describes the measurement setup and the common elements of the employed methodology. Section III describes the specific processing utilized in the analysis of each noise term, provides representative examples and summarizes their main characteristics. Concluding remarks are given in section IV.

## II. Measurement Methodology

The measurement setup consists of a PC with a 12 bits data acquisition card (DAC). It has a configurable dynamic range and an input impedance of 50 Ω. The DAC is plugged to the power network outlets through a coupling circuit that acts as a passband filter and as a balun that extracts differential mode signal. The measured bandwidth extends up to 25 MHz. The captured data is real-time transferred to the PC, allowing recording lengths equivalent to hundreds of mains cycles.

The performed analysis combines time-domain and frequency-domain techniques. Although the signal processing algorithms used in each case depend on the particularities of the noise component under analysis, a high resolution spectral analysis based on periodogram averaging is employed in all cases. Because of the cyclostationary nature of most noise terms, this averaging is performed in a cyclic way. Let's denote by $T_o$ the mains period and by $T_s$ the sampling period, which is selected to be a submultiple of $T_o$. The output signal from the coupling circuit, $x(n)$, is registered during the time of $C$ mains cycles. Each mains cycle, $c$, whose nominal length is $N_C = T_o/T_s$ samples, and whose equivalent time jitter is $\tau(c)$ samples, is also divided into $L$ intervals with $N_L = \left\lfloor \frac{T_o}{T_s L} \right\rfloor$ samples. Hence, the captured signal during the $\ell$th interval of the $c$th cycle can be written as

$$x_{c,\ell}(n) = x(n + cN_c + \sum_{i=0}^{c} \tau(i) + \ell N_L), \qquad (1)$$

with $0 \leq n \leq N_L - 1$. The corresponding periodogram is then computed according to

$$P_c(\ell, k) = \frac{1}{UN_L} \left| \sum_{n=0}^{N_L-1} w(n) x_{c,\ell}(n) e^{-j\frac{2\pi}{N_L}kn} \right|^2, \qquad (2)$$

where $w(n)$ is a Hanning window of $N_L$ samples and $U$ is the normalization factor that removes the estimation bias [12]. An estimate of the time and frequency sampled version of the noise instantaneous PSD can then be obtained by performing a synchronized averaging of the

periodograms in (2)

$$\widehat{S}_N(\ell,k) = \widehat{S}_N(t,f)\big|_{t=\ell T_s N_L, f=\frac{k}{T_s N_L}} = \frac{1}{C}\sum_{c=0}^{C-1} P_c(\ell,k), \tag{3}$$

where $C = 234$ and $N_L = 2^{16}$, leading to a time and frequency resolution of approximately 1.3 ms and 3 kHz, respectively.

The estimated instantaneous PSD in (3) is used as the starting point for the analysis of all noise terms. The next section describes the specific signal processing employed in each case, along with representative results and a summary of their main characteristics.

## III. Measurements Results

### A. Periodic Impulsive Noise Synchronous with the Mains

This noise component manifests itself in a twofold manner: as a series of isolated impulses of considerable duration (up to hundreds of microseconds) and amplitude, and as impulse trains that always appear in the same instant of the mains cycle but in which the number of impulses and separation between them varies from cycle to cycle. These impulses use to be shorter and with lower amplitude than the first ones. However, both of them appear with a repetition rate of 50 Hz/100 Hz (in Europe). From now on, the former term will be referred to as type 1 and the latter as type 2. Fig. 1 depicts the time-domain representation of the noise registered in an apartment with a detailed view of the aforementioned components. The increase in the noise level that occurs around 5 ms and 15 ms are caused by two synchronous narrowband interferences.

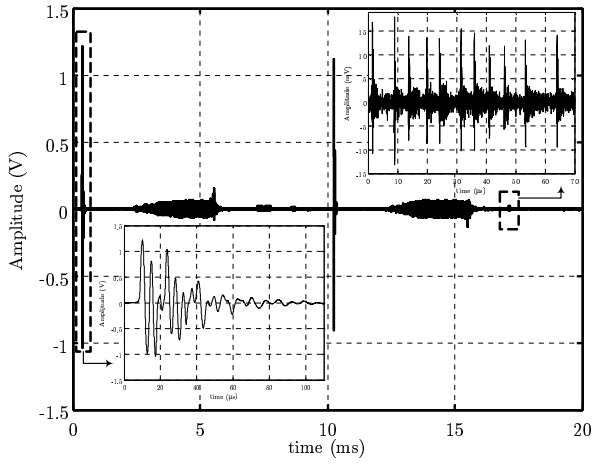


Fig. 1. Noise registered in an apartment during one mains cycle with detailed view of the periodic synchronous impulsive components.

The procedure employed to obtain pulse waveforms makes use of the estimated instantaneous PSD in (3). Their position within the mains cycle is detected by identifying significant and frequency localized variations of the level in successive intervals of $\widehat{S}_N(\ell,k)$, since the resolution of the spectral analysis is insufficient to appreciate the harmonics due to the 50 Hz/100 Hz periodicity. Pulses are then extracted by performing a multiband filtering over the corresponding interval. Finally, the periodic behavior is verified by correlating them with the overall noise register.

As stated before, type 1 impulses usually have large amplitudes. However, the presented procedure is able to obtain pulses with similar level to the remaining noise terms. Fig. 2(a) shows the pulse waveform, $p(t)$, of a type 1 periodic synchronous impulse obtained with the proposed methodology and Fig. 2(b) depicts the corresponding Energy Spectral Density (ESD), defined as

$$ESD(f) = 20\log_{10}\left(|P(f)|\right) \quad \text{(dBV)}, \tag{4}$$

where $P(f)$ is the Fourier Transform of $p(t)$ in volts.

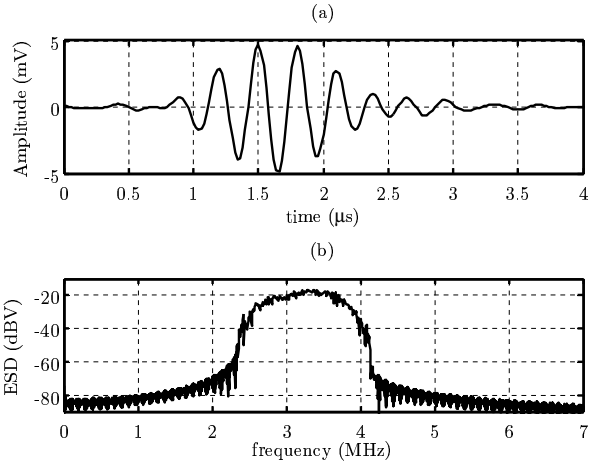


Fig. 2. Pulse waveform (a), and ESD of a type 1 periodic synchronous impulse measured in a detached house (b).

Measurements accomplished in this work reveal that periodic synchronous impulsive noise terms exhibit remarkable disparity between locations. Table I summarizes their main characteristics. It is interesting to note that, from a communication system perspective, type 2 is generally the most harmful term, despite its lower amplitude, since type 1 impulses are usually located below 1MHz.

TABLE I
SUMMARY OF THE PERIODIC SYNCHRONOUS IMPULSIVE NOISE CHARACTERISTICS

| Parameter | Type 1 | Type 2 |
|---|---|---|
| Number of impulses within a mains cycle | less than 10 | less than 10 |
| Duration | from 2 $\mu$s up to 300 $\mu$s | train duration up to 500 $\mu$s and impulse duration smaller than 1 $\mu$s |
| Amplitude | from 5 mV up to 1.5 Volt | less than 50mV |
| Central frequency | typically below 500 kHz, occasionally up to 3 MHz | up to 7 MHz |
| Bandwidth | typically below 250 kHz, occasionally up to 2 MHz | up to 11 MHz |

### *B. Periodic Impulsive Noise Asynchronous with the Mains*

This noise component takes the form of short duration impulse trains that always appear at the same instants of the mains cycle. Repetition rates range from approximately 12 kHz up to 217 kHz. Since the frequency resolution of the spectral analysis is about 3 kHz, these noise terms manifest in the instantaneous PSD as very narrow peaks. To obtain the pulse waveforms and the repetition rates, a spectral mask, $M_\ell^i(k)$, that identifies all the spectral peaks due to the $i$th periodic asynchronous component of the $\ell$th interval is determined according to the algorithm described in [13]. Given that $M_\ell^i(k) = 1$ if the corresponding asynchronous noise term has a spectral peak in $k$ and zero elsewhere, the pulse waveform can be obtained as

$$p_i(n) = \text{IDFT}\left\{M_\ell^i(k)\text{DFT}\left\{x_{c,\ell}(n)\right\}\right\}, \qquad (5)$$

where $\text{DFT}\{\cdot\}$ and $\text{IDFT}\{\cdot\}$ denote the $N_L$-point Discrete Fourier Transform and Inverse DFT, respectively.

This procedure is able to retrieve pulse waveforms with such low amplitude that would be undetectable with the traditional measurement procedure based on a digital oscilloscope triggered by a peak detector. Fig. 3 shows an example of this situation. Fig. 3(a) depicts a small interval of the noise captured in an apartment. The y-axis has been scaled according to the amplitudes registered during the first 1.3 ms. This makes difficult to notice that the term around 1.5 ms is a high amplitude periodic impulse synchronous with the mains. As seen, there is no visual trace of any periodic asynchronous impulsive component. However, the estimated PSD for this interval, shown in Fig. 3(b), clearly reveals its presence. The proposed methodology gives the pulse waveform drawn in Fig. 4, which consists of a set of two impulses with a repetition rate of 70 kHz.

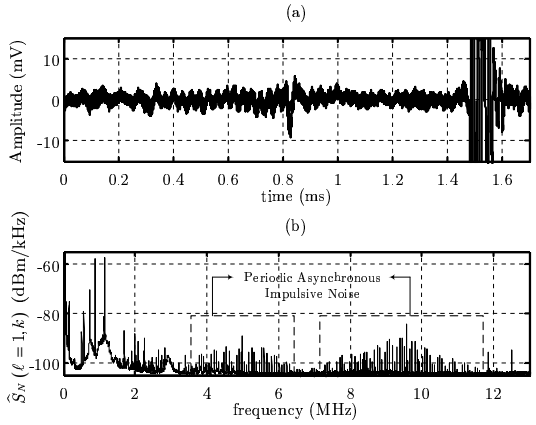


Fig. 3. Time-domain representation of the noise registered in an apartment (a), and estimated PSD of the first 1.3 ms (b).

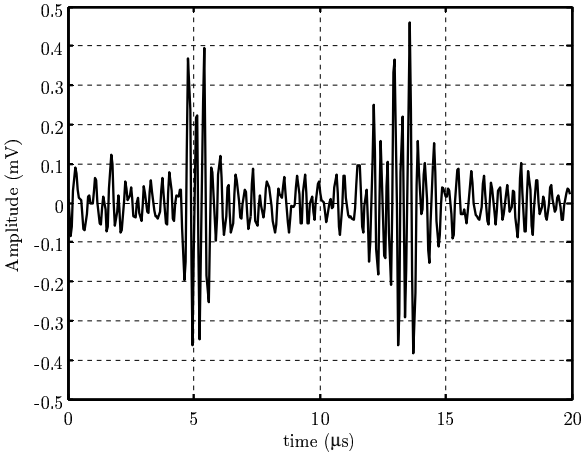


Fig. 4. Pulse waveform of the periodic asynchronous noise existing in the noise register shown in Fig. 3.

Fig. 5(a) depicts an example of a low repetition rate periodic asynchronous impulsive noise registered in a university laboratory. It is basically composed of two short pulses (duration around 1 $\mu$s) that alternate their polarity once per period. The repetition rate of this component is 26.3 kHz, which is quite below the range typically assigned in the literature to this noise type. Fig. 5(b) shows the ESD corresponding to the first impulse in Fig. 5(a).

Fig. 6 shows an example of a periodic asynchronous impulsive noise with high frequency components. Fig.

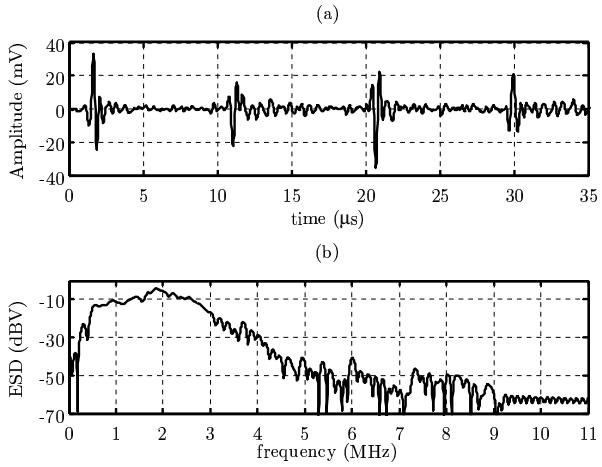


Fig. 5. Time-domain representation of a low repetition rate periodic asynchronous impulsive noise (a), and ESD of the first impulse (b).

6(a) depicts the time-domain waveform, which is composed of a higher amplitude and a low amplitude pulse that repeats with 48.93 kHz, and Fig. 6(b) shows the corresponding ESD.

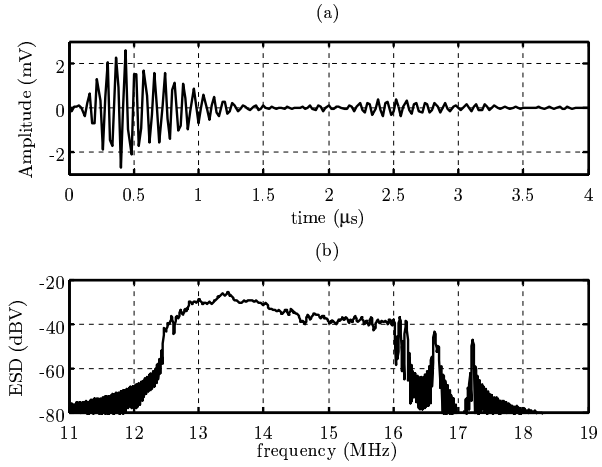


Fig. 6. Time-domain representation (a), and ESD of a periodic asynchronous impulsive noise with high frequency components (b).

Periodic asynchronous impulse terms usually appear only in certain instants of the mains cycle. Although there are a great variety of behaviors, a common appearance pattern is composed of two impulse trains symmetrically located within the mains cycle. A pattern in which the trains appear both in the vicinity of the zero crossings, the minimum and the maximum values of the mains is also typical. Situations in which some noise components are present during the whole mains cycle but with different amplitudes have been also found [13]. In all cases, impulses are generally present in at least 50% of the mains cycle duration. Table II summarizes the main characteristics of the measured periodic asynchronous impulsive noise.

TABLE II
SUMMARY OF THE PERIODIC ASYNCHRONOUS IMPULSIVE NOISE CHARACTERISTICS

| Parameter | Value |
|---|---|
| Number of different components in a mains cycle | one or none in weakly disturbed scenarios and more than 3 in highly disturbed ones |
| Appearance pattern | present all the time, 2 states (on/off) per mains cycle, 4 states (on/off) per mains cycle & others |
| Duration | typically less than 1.5 $\mu$s, occasionally up to 10 $\mu$s |
| Amplitude | typically less than 4 mV, occasionally up to 40 mV |
| Repetition rates | 12.6 kHz, 15.6 kHz, 26.3 kHz, 48.9 kHz, 56.5 kHz, 59.1 kHz, 70 kHz, 90.1kHz and 217.2kHz |
| Central frequency | from 2 MHz up to 13 MHz |
| Bandwidth | from 2 MHz up to 9 MHz |

### C. Sporadic Impulsive Noise

This is the most unpredictable impulsive noise term. Two types of sporadic components have been observed. The first one consists of isolated impulses with considerable amplitudes and widths, and from now on will be referred to as type 1. The second one takes the form of impulse trains with arbitrary separation between the constituent pulses, and from now on will be denoted as type 2. These pulses use to have lower amplitude and smaller duration than those of the first type.

In all cases, those intervals of the mains cycle containing these noise types have larger energy than the remaining ones. Hence, the procedure employed to detect them divides the mains cycle into $L$ intervals and computes their energy, leading to

$$E(c,\ell) = \sum_{n=0}^{N_L-1} |x_{c,\ell}(n)|^2 . \qquad (6)$$

Then, high energy intervals that do not appear in successive cycles are searched.

Fig. 7 depicts results obtained when computing the energy of 100 mains cycles divided into $L = 15$ intervals. As seen, cyclostationary noise components are clearly identifiable by the vertical stripes around 0 ms, 8 ms and 18ms. A type 1 sporadic impulsive noise with very

high energy can be observed around 16ms in the 64th cycle. Fig. 8 displays the corresponding pulse waveform and its ESD.

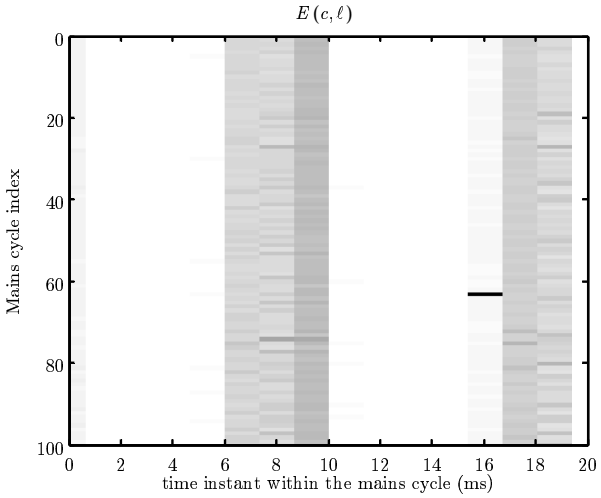


Fig. 7. Spectrogram of the energy computed over 100 mains cycles with $L = 15$ intervals per mains cycle.

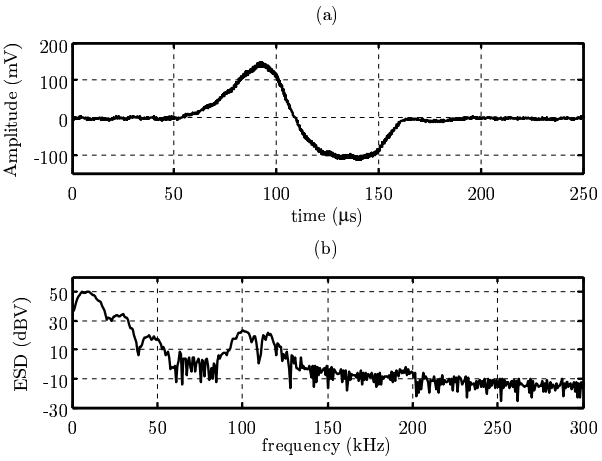


Fig. 8. Time-domain representation (a), and ESD (b), of the sporadic impulsive noise identified in Fig. 7.

Fig. 9 shows an example of the type 2 sporadic impulsive noise. Fig. 9(a) displays the impulse train, Fig. 9(b) shows a detail of the impulse with higher amplitude (although all of them have essentially the same waveform) and Fig. 9(c) depicts its ESD. As seen, type 2 impulses use to have lower amplitude and higher frequency components. Table III summarizes the main characteristics of both sporadic noise types.

Previous analyses, in which interarrival and amplitude distributions are computed without differentiating between the two periodic noise terms, show that impulses with greater width and amplitude have higher probability in weakly disturbed scenarios [7]. This can be easily explained according to the results presented in this work. Thus, measurements indicate that the difference between weakly and highly disturbed scenarios is essentially due to the background noise level and to the number of periodic asynchronous impulsive components. Sporadic impulses and periodic synchronous terms are generally the only impulsive components in weakly disturbed environments. Hence, according to data presented in Table I-III, most of the impulses registered in these situations have large amplitude and duration.

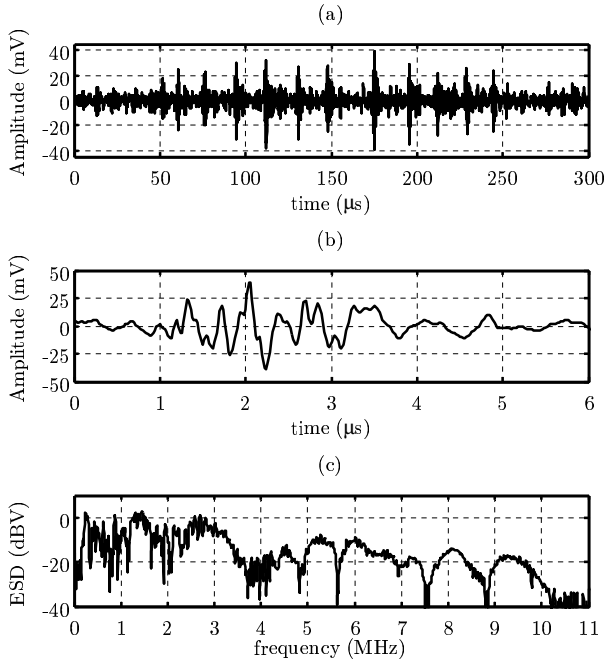


Fig. 9. Time-domain representation (a)-(b), and ESD of a type 2 sporadic impulsive noise (c).

TABLE III
SUMMARY OF THE SPORADIC IMPULSIVE NOISE CHARACTERISTICS

| Parameter | Type 1 | Type 2 |
|---|---|---|
| Duration | from 15 $\mu$s up to 150 $\mu$s | less than 20 $\mu$s |
| Amplitude | from 20 mV up to 150 mV | from 3 mV up to 50 mV |
| Central frequency | typically below 1 MHz | up to 7 MHz |
| Bandwidth | typically below 1 MHz | up to 11 MHz |

### D. Narrowband Interferences

This disturbance type is easily detected in the estimated instantaneous PSD because of its significant level over the background noise and, in general, over the remaining noise terms. They can be classified according to the shape of their PSD into the following categories:

1) *Interferences with multiple discrete frequency components.* The PSD of these interferences consists of several equally spaced narrowband components (less than 5 kHz bandwidth). However, contrary to the peaks due to periodic asynchronous terms, they are not harmonically related, i.e. denoting by $f_j$, with $j = 0, 1, ...$, the frequencies of the spectral peaks, it happens that $f_j - f_{j-1} = f_{j+1} - f_j$ but there is no $f_0$ that satisfies $f_j = pf_0$, for $j = 0, 1, ...$ and $p \in \mathbb{N}^+$. They are usually located above 4 MHz and frequency spacings up to 50 kHz have been observed. Fig. 10(a) shows the estimated PSD of an interference of this type. As seen, it has the shape of the DSB (Double Side Band) modulation of a periodic signal. Fig. 10(b) depicts its corresponding time-domain waveform, obtained by applying a bandpass filter to the noise register.
2) *Interferences with one frequency component.* The PSD of these interferences consists of a single narrowband term (bandwidth below 20 kHz) and a significant level over the background noise (even more than 30dB). They can be typically found below 2 MHz and above 20 MHz. Interferences from commercial AM (Amplitude Modulation) radio stations are an example of this category.

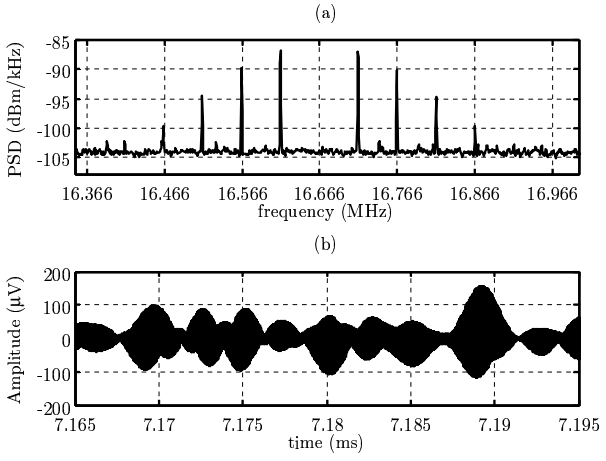


Fig. 10. PSD of an interference with multiple discrete frequency components (a), and its corresponding time-domain waveform (b).

Alternatively, interferences can be classified according to their statistical properties into:

1) *Stationary.* They can be composed of multiple equally spaced narrowband components or just a single term, but their levels do not change along the mains cycle. Most of the registered interferences fall within this group.
2) *Cyclostationary.* These interferences can be also composed of multiple frequency terms or a single one. However, their distinctive feature is their synchronous character with the mains. Fig. 10 shows the time-domain representation of a noise register that contains this type of interference. It depicts the detailed view of a 76 kHz cyclostationary narrowband interference that appears just before the two periodic synchronous impulses with highest amplitude. The superimposed effect of an AM interference with a carrier frequency of 882 kHz and smaller amplitude can be also observed. The cyclostationary behavior of the 76 kHz interference is corroborated by the zoomed region around 8ms, where only the AM interference is present. As shown in Fig. 10, these interferences usually precede the periodic synchronous impulses.

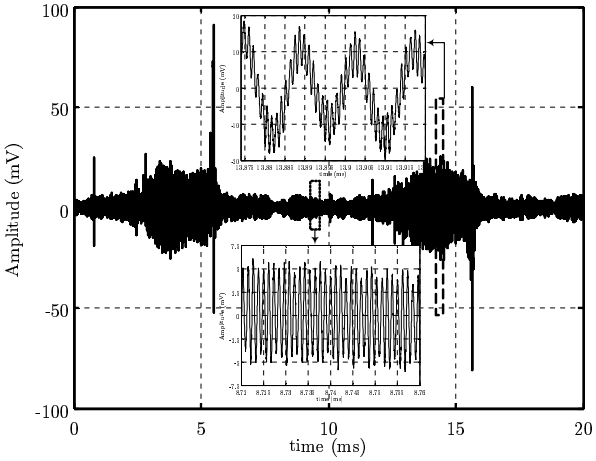


Fig. 11. Noise registered in an apartment during one mains cycle with detailed view of two narrowband interferences.

### E. Background Noise

The analysis of the cyclostationary background noise is aimed to estimate its instantaneous PSD, $\widehat{S}_{BN}(\ell, k)$. To this end, the spectral peaks caused by the periodic asynchronous impulsive noise components and the narrowband interferences must be removed. This objective is achieved by applying the following algorithm to each time interval $\ell$:

1) *Estimate the instantaneous PSD of the registered noise*. An estimate of the noise instantaneous PSD, $\widehat{S}_N(\ell,k)$, is obtained according to (3). The number of time intervals, $L$, determines the time and frequency resolution of the estimation. Its selection involves the following trade-off. An excessively high value of $L$ results in a poor frequency resolution that veils the presence of the periodic asynchronous noise terms. On the other hand, an excessively low value of $L$ leads to a poor time resolution, causing cyclostationary interferences and periodic synchronous noise components to overestimate the background noise level. An appropriate value is $L = 15$, which leads to a time and frequency resolution of 1.3 ms and 3 kHz, respectively.
2) *Determine the set of frequencies corresponding to the spectral peaks in* $\widehat{S}_N(\ell,k)$. Denoting by $k_\ell^i$, with $i = 0, 1, ...$, the frequencies where $\widehat{S}_N(\ell,k)$ has a spectral peak, the output of this phase is the set $K_\ell = \{k_\ell^0, k_\ell^1, ...\}$.
3) *Eliminate the spectral peaks in* $\widehat{S}_N(\ell,k)$. The objective of this step is to generate a new PSD, $\widetilde{S}_N(\ell,k)$, equal to $\widehat{S}_N(\ell,k)$ but with no trace of the spectral peaks due to the narrowband interferences and to the periodic asynchronous impulsive components. To this aim, the values of $\widehat{S}_N(\ell,k)$ for $k \in K_\ell$ are replaced by the minimum value taken by $\widehat{S}_N(\ell,k)$ in an interval centered in $k$,

$$\widetilde{S}_N(\ell,k) = \begin{cases} \widehat{S}_N(\ell,k) & k \notin K_\ell \\ \min\limits_{\kappa=k-W/2...k+W/2} \left\{ \widehat{S}_N(\ell,\kappa) \right\} & k \in K_\ell. \end{cases} \quad (7)$$

The interval length, $W$, is fixed to obtain an equivalent bandwidth of 30 kHz, approximately.
4) *Smooth the staircase behavior of* $\widetilde{S}_N(\ell,k)$. The processing in (7) gives a staircase behavior to $\widetilde{S}_N(\ell,k)$ in the vicinity of $k \in K_\ell$. To remove it, a weak low-pass filter is applied to $\widetilde{S}_N(\ell,k)$, yielding to an estimation of the background noise, $\widehat{S}_{BN}(\ell,k)$.

Fig. 12 depicts the $\widehat{S}_N(\ell,k)$ of the noise registered in a university laboratory. It corresponds to a heavily disturbed scenario, with a lot of periodic asynchronous components. A zoom of the frequency band between 6 MHz and 7 MHz has been included to appreciate them. Fig. 13 shows the values of $\widehat{S}_{BN}(\ell,k)$ corresponding to the PSD shown in Fig. 12. Additionally, the estimates of the background noise obtained in a detached house and in an apartment have been also included. As seen, the background noise PSD of the noise registered in the university laboratory does not fit the simple exponential models proposed in previous works [4], [14]. These models are appropriate for weakly disturbed scenarios and, in some cases, for medium disturbed ones. However, they do not capture the spectral richness of the noise existing in highly disturbed environments.

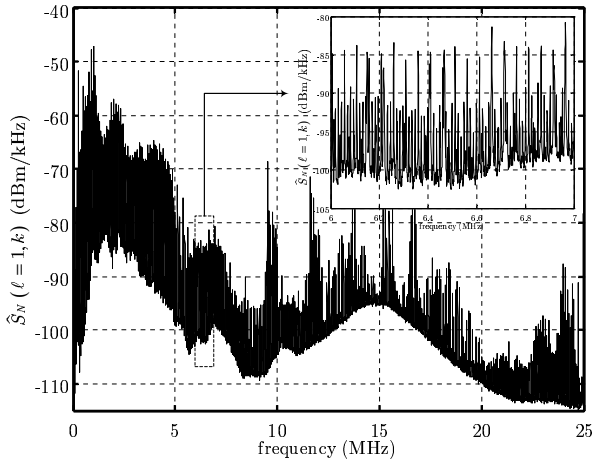


Fig. 12. Estimated PSD of the noise registered in a university laboratory.

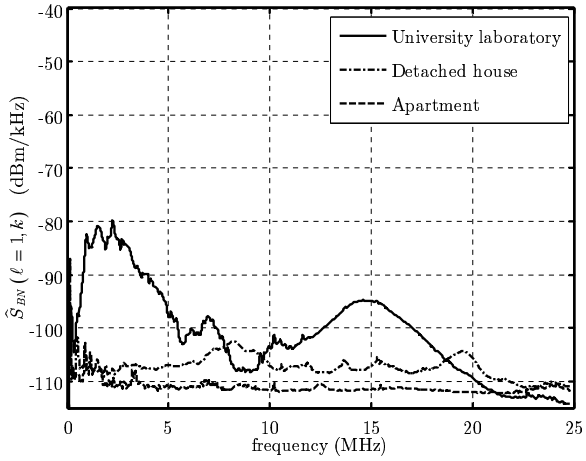


Fig. 13. Background noise PSD obtained from Fig. 12, and from the noise registered in a detached house and in an apartment.

The cyclostationary nature of the background noise can be observed in Fig. 14. It depicts the estimated PSD of the background noise registered in a university laboratory. This cyclostationary behavior has been observed in all the scenarios. However, it has been more frequently found, and with higher level differences, in highly disturbed environments.

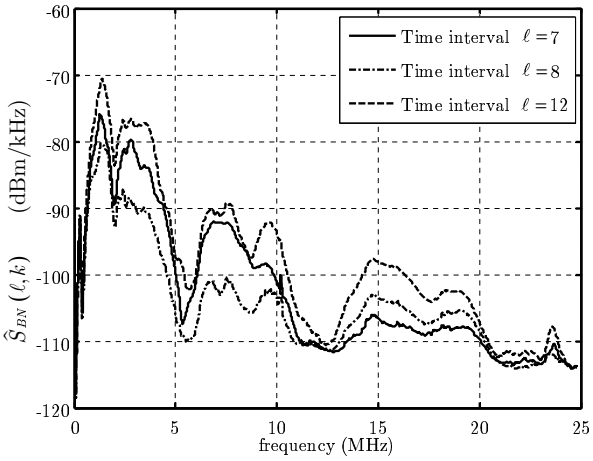


Fig. 14. Estimated PSD of the background noise registered in a university laboratory.

The presented algorithm cannot be applied to estimate the background noise PSD of those intervals with periodic synchronous impulsive noise, since the operation in (7) does not remove them from the PSD because of the insufficient resolution of the spectral analysis. However, this is not a serious impairment because these impulses are time-localized and occupy only a small percentage of the mains cycle.

### *F. Noise Probability Density Function*

According to the noise components described up to now, it is clear that broadband PLC noise does not have a Gaussian nature. This fact has been already reported in the literature [4] and contrasts with published results for narrowband PLC noise [15], where the noise is said to have a Gaussian distribution.

The method employed in this work to estimate the noise PDF divides the mains cycle into $L$ intervals. However, to obtain a higher time resolution, $L$ is fixed to a much higher value than in previous sections: $L = 976$. The estimated PDF of the $\ell$th interval is then obtained from the samples of $x_{c,\ell}(n)$ for $c = 0...C-1$. Fig. 15 shows some of the PDFs estimated over the noise register acquired in a detached house. A Gaussian PDF of the same variance is also included for reference. PDFs exhibiting higher probabilities than a normally distributed variable for extreme values correspond to intervals with impulsive noise components. However, it is worth noting that in those intervals with no trace of these noise components, the obtained PDF is indistinguishable from the Gaussian one. Hence, it can be concluded that the background noise is Gaussianly distributed.

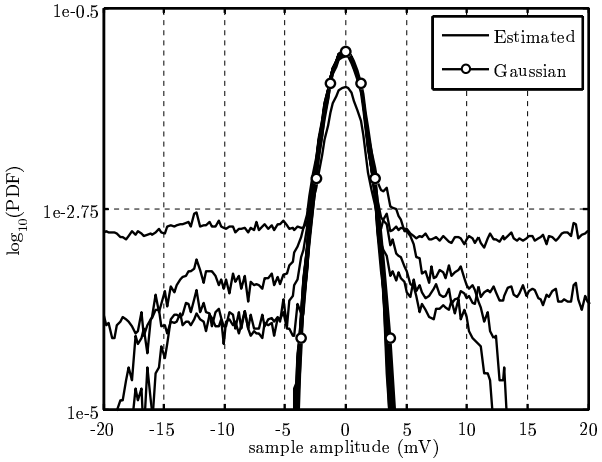


Fig. 15. Estimated PDFs of the noise registered in a detached house at different time intervals.

## IV. Conclusion

This paper has presented a detailed analysis of the indoor broadband power-line noise components. The employed methodology combines time-domain techniques with a high resolution spectral analysis based on periodogram averaging that captures the cyclostationary nature of most noise terms. The study relies on a measurement campaign performed over more than 50 noise registers in three different scenarios.

Concerning the impulsive noise, it has been shown that periodic synchronous terms have a twofold nature: a series of isolated impulses, of considerable duration and amplitude, and impulse trains that always appear in the same instant of the mains cycle but in which the number of impulses and separation between them varies from cycle to cycle. These impulses use to be shorter and with lower amplitude than the first ones. Except for the latter type, periodic synchronous components use to occupy the frequency band below 1 MHz. Similarly, the analysis of the periodic asynchronous noise has revealed that they also exhibit a synchronous behavior with the mains. Repetition rates from 12.6 kHz up to 217.2 kHz have been measured. Similarly, a procedure to extract sporadic impulsive noise, which is the most unpredictable term, has been presented. Examples of pulse waveforms and their corresponding energy spectral densities have been given in all cases.

A classification of the narrowband interferences according to their PSD and their statistical behavior has been also given. It has been shown that some of them

exhibit a cyclostationary behavior. Finally, a procedure to compute the background noise power spectral density has been presented. It has been demonstrated that the classical exponential model does not captures the spectral richness of the heavily disturbed scenarios. It has been also shown that, according to the accomplished measurements, the background noise has a Gaussian distribution.

## ACKNOWLEDGMENT

This work has been partially supported by the Spanish MEC under Project TIC2003-06842.

## REFERENCES

[1] H. Philipps, "Performance measurements of power-line channels at high frequencies," in *Proceedings of the International Symposium on Power Line Communications and its Applications (ISPLC)*, 1998, pp. 229–237.

[2] F. J. Cañete, J. A. Cortés, L. Díez, and J. T. Entrambasaguas, "Analysis of the cyclic short-term variation of indoor power line channels," *IEEE Journal on Selected Areas on Communications*, vol. 24, no. 7, pp. 1327–1338, July 2006.

[3] F. J. Cañete, L. Díez, J. A. Cortés, and J. T. Entrambasaguas, "Broadband modelling of indoor power-line channels," *IEEE Transactions on Consumer Electronics*, pp. 175–183, Feb 2002.

[4] T. Esmailian, F. R. Kschischang, and P. G. Gulak, "In-building power lines as high-speed communication channels: channel characterization and a test channel ensemble," *International Journal of Communications*, vol. 16, pp. 381–400, June 2003.

[5] S. Galli and T. C. Banwell, "A deterministic frequency-domain model for the indoor power line transfer function," *IEEE Journal on Selected Areas on Communications*, vol. 24, no. 7, pp. 1304–1316, July 2006.

[6] Y. Hirayama, H. Okada, T. Yamazato, and M. Katayama, "Noise analysis on wide-band PLC with high sampling rate and long observation time," in *Proceedings of the International Symposium on Power Line Communications and its Applications (ISPLC)*, 2003, pp. 142–147.

[7] M. Zimmermann and K. Dostert, "Analysis and modeling of impulsive noise in broad-band powerline communications," *IEEE Transactions on Electromagnetic Compatibility*, vol. 44, no. 1, pp. 249–258, February 2002.

[8] V. Degardin, M. Lienard, A. Zeddam, F. Gauthier, and P. Degauque, "Classification and characterization of impulsive noise on indoor power line used for data communications," *IEEE Transactions on Consumer Electronics*, vol. 48, no. 4, pp. 913–918, November 2002.

[9] D. Liu, E. Flint, B. Gaucher, and Y. Kwark, "Wide band AC power line characterization," *IEEE Transactions on Consumer Electronics*, vol. 45, no. 4, pp. 1087–1097, November 1999.

[10] H. Meng, Y. L. Guan, and S. Chen, "Modeling and analysis of noise effects on broadband power-line communications," *IEEE Transactions on Power Delivery*, vol. 20, no. 2, pp. 630–637, April 2005.

[11] R. García, L. Díez, J. A. Cortés, and F. J. Cañete, "Mitigation of cyclic short-time noise in indoor power-line channels," in *Proceedings of the IEEE International Symposium on Power Line Communications and Its Applications (ISPLC)*, March 2007, pp. 396–400.

[12] A. Oppenheim, R. Schafer, and J. Buck, *Discrete-time Signal Processing*. Prentice Hall, 1999.

[13] J. A. Cortés, L. Díez, F. J. Cañete, and J. López, "Analysis of the periodic impulsive noise asynchronous with the mains in indoor PLC channels," in *Accepted for publication in the IEEE International Symposium on Power Line Communications and its Applications*, March-April 2009.

[14] D. Benyoucef, "A new statistical model of the noise power density spectrum for powerline communication," in *Proceedings of the International Symposium on Power-Line Communications and its Applications (ISPLC)*, March 2003, pp. 136–141.

[15] M. Katayama, T. Yamazato, and H. Okada, "A mathematical model of noise in narrowband power line communication systems," *IEEE Journal on Selected Areas on Communications*, vol. 24, no. 7, pp. 1267–1276, July 2006.